Accurate reference ionospheric model for testing GNSS ionospheric correction in EGNOS and Galileo

J.M. Juan*, J. Sanz*, G. González-Casado*, A. Rovira-Garcia*, D. Ibáñez*
R. Orús†, R. Prieto-Cerdeira†, S. Schlüter‡

*Research Group of Astronomy and Geomatics, Technical University of Catalonia, gAGE/UPC, Barcelona, Spain
jose.miguel.juan@upc.edu, jaume.sanz@upc.edu, guillermo.gonzalez@upc.edu, adria.rovira@upc.edu, dibanez@ma4.upc.edu

†European Space Agency, ESA, Noordwijk, The Netherlands
raul.orus.perez@esa.int, roberto.prieto.cerdeira@esa.int

‡EGNOS Project Office, EPO, Toulouse, France
stefan.schlueter@esa.int

Abstract

This work presents a procedure to assess ionospheric models tailored for Global Navigation Satellite System (GNSS) applications. The test is based on actual carrier-phase measurements. Using this strategy, the accuracy of the ionospheric broadcast models for Global Positioning System (GPS), Galileo and the European Geostationary Navigation Overlay System (EGNOS) is assessed. These models are compared to the Global Ionospheric Maps (GIMs) from the International GNSS Service (IGS) and a new product developed by the Research group of Astronomy and Geomatics (gAGE/UPC). The accuracies of the different ionospheric estimates are shown to affect the satellite and receiver Differential Code Bias (DCB) estimations. An accurate enough ionospheric modelling is shown to be able to detect actual drifts occurring in permanent receivers.

I. Introduction

Typical consumer mass-market receivers are single-frequency. The Standard Point Positioning (SPP) user corrects the GNSS observations with the ionospheric delays predicted by a broadcast model. Therefore, the performance of the navigation solution will depend, among other factors, on the accuracy of the ionospheric model chosen.

The characterization of the accuracy of ionospheric models for GNSS is a well-known challenging problem. A correct assessment is crucial as a first step for improving current models. But, any testing process requires confident enough ionospheric determinations to be used as a reference. How to derive such reference values for the ionospheric delays is not a fully solved problem.

Several attempts have been done in this direction. For instance, simulated data sets have been extensively used to assess the performance of ionospheric models. However, the main problem when simulations are used is their limited degree of realism to reproduce perturbed (i.e., non-nominal) ionospheric conditions. Events quite ordinary such as geomagnetic storms in northern latitudes or equatorial scintillation after the local sunset are difficult to be realistically simulated.

Other tests directly use the Total Electron Content (TEC) measurements from dual-frequency space-borne radar altimeters like TOPEX/Jason [1]. Although this data is independent, it presents some practical disadvantages. First, the orbit height of such satellites is about 1300 kilometres [2], so it is unable to sample the upper part of the ionospheric delay which extends several hundreds of kilometres above. Second, the biases present at the satellite are not well calibrated. Third, the measurements are limited to the ice-free oceans and present a noise several times greater than the GNSS measurements. Therefore, it is difficult to distinguish which part of the error is due to the ionospheric model under test and which is due to the radar-altimeter data.

In this work, we use actual dual-frequency GNSS code and carrier-phase measurements from more than 100 receivers world-wide distributed, to derive ionospheric delays estimates with an Root Mean Square (RMS) accuracy at the level or better than 1 Total Electron Content Unit (TECU) (16 cm in L1 frequency). This accuracy is required in the context of the ICASES [3] projects. This performance is achieved thanks to the joint processing of all the GNSS measurements in an unique Central Processing Facility (CPF), developed by the Research group of Astronomy and Geomatics (gAGE/UPC), that combines geodesy and ionospheric modelling.

Indeed, the usual geodetic parameters are estimated (satellite orbits and clocks, receiver clocks, tropospheric delays, carrier phase ambiguities...) using the non-dispersive combination of observables. The CPF satellite orbit and clock accuracies are

comparable [4] with the Real-Time Pilot Project (RTPP) [5] combined product of the International GNSS Service (IGS) [6]. In this way, the non-dispersive part of the carrier-phase measurements are accurately modelled up to the centimetre level, this allows the carrier-phase ambiguities to be fixed.

Thence, the accuracy of the geodesy estimated parameters is transferred to the ionospheric determinations. Using these fixed carrier-phase ambiguities, the dispersive combinations of observables can be modelled at the level of few centimetres in undifferenced mode, and much better in differenced mode. This synergy is used to derive a highly-accurate ionospheric model together with the Differential Code Bias (DCB) for satellites and receivers.

This work is divided as follows. Section II reviews the different ionospheric models which are assessed in this work, including details of the how the precise gAGE/UPC ionospheric model is derived. Section III presents a procedure to assess any ionospheric model for GNSS applications. This test has been routinely applied for 6 months from February 1, 2014. Results are divided according to the region; global results and regional (Europe) are presented in Section IV and Section V, respectively. Section VI presents an analogous strategy to assess the DCB. Section VII compares the accuracy of estimating the satellite and receiver DCB using different ionospheric determinations, because such biases are affected [7] by the geometric description of the ionosphere. Section VIII provides an additional usage of the precise ionospheric modelling achieved by the gAGE/UPC, where an actual drift on an IGS station DCB can be detected. Last section summarizes the results.

II. Ionospheric Model Descriptions

The ionospheric models used nowadays in GNSS present significant differences on its main characteristics which determine their performance. Thence, it is worthy to briefly describe the ionospheric models that will be tested later in this work.

A. Fast-PPP Ionospheric Model

It is the ionospheric model developed by the authors for the Fast Precise Point Positioning (Fast-PPP) technique (see [8] for a description of the architecture), which is able to provide high-accuracy navigation quickly. It is based on the accurate modelling at the centimetre level of the wide-lane and ionosphere-free combination [9] of carrier-phases. Once the ambiguities of these combinations (BW and BC, respectively) are well-estimated, they can be fixed to integer values. The gAGE/UPC CPF transfers the accuracy of the geodesy estimates to the ionospheric modelling by building the carrier-phase ambiguity in the geometry-free combination ($BI = B1 - B2$) using the relation:

$$BI = \frac{1}{\alpha_w}(BW - BC) \tag{1}$$

Where the frequency factor $\alpha_w = (f_1 f_2)/(f_1^2 - f_2^2)$ is 1.98 for the GPS frequencies L1 and L2 used in this work. Thence, by subtracting this ambiguity to the geometry-free combination of carrier-phases ($LI = L1 - L2$), one can have a very precise sampling of the Slant Total Electron Content (STEC) present in the measurements between any satellite j and any receiver i (see [9] for the notation details):

$$LI_i^j - BI_i^j = STEC_i^j + DCB_i - DCB^j \tag{2}$$

It was early pointed in [7], that the ionospheric delay term, $STEC_i^j$ can be distinguished from a constant part; the satellite DCB^j and receiver DCB_i. The gAGE/UPC ionospheric model accurately estimates every 5 minutes each slant ionospheric delay $STEC_i^j$ using a lineal combination of the vertical ionospheric delays ($VTEC_k$) on a set of Ionospheric Grid Points (IGPs). These IGPs are distributed in two layers using a constant resolution of 250 and 500 kilometres in both latitude and longitude, in the first and second layer, respectively:

$$STEC_i^j = \sum \alpha_k \cdot VTEC_k \tag{3}$$

Where α_k is a factor which includes the mapping function (i.e., obliquity factor) and the interpolation from the IGPs to the satellite Ionospheric Pierce Point (IPP). The two-layer model [10] separates the main ionosphere (at low height) from the plasmasphere (the upper component), placing the layers at 270 km and 1600 km in height, respectively. This is particularly important in low latitude regions, as shown in Section IV.

The precise input data and the adequate geometry used, make the Fast-PPP model consisting and projecting the STEC delays on vertical values on the IGPs, for this reason the error in the test should reflect the projection and de-projection losses, if any.

B. Fast-PPP Global Ionospheric Model

The gAGE/UPC GIMs are build from the Fast-PPP ionospheric model, which is only available to regions where IGPs are sampled by GNSS observations in real time. For instance, the formal errors of the model are very large in oceans or other poorly sounded regions. To provide a global coverage, as required for the ICASES [3] project, all IGPs must be estimated. For this purpouse, a smoothing process (in post-process) is applied which includes a backward estimation of the Vertical Total Electon Content (VTEC) at the IGPs. This procedure covers all the region at a cost of partially degrading the well-sounded IGPs. The time resolution of these maps is 15 minutes.

C. Klobuchar model

This is the well-known ionospheric model [11] used by GPS and BeiDou Navigation Satellite System (BDS). The model assumes the ionospheric delays occur at a thin layer at a height of 350 km in GPS and 375 km in BDS. The model predictions are driven by a set of 8 parameters included in the navigation message of each constellation. These coefficients are updated typically once a day.

D. NeQuick G model

It is the ionospheric model [12] implemented in the Galileo receivers. The model is driven by a single parameter (i.e., the effective ionisation level A_z), which depends on the MOdified DIP latitude (MODIP) of the satellite IPP at 300 km height. This dependency is modelled with a second order polynomial with 3 coefficients that are broadcast in the Galileo navigation message, and updated at least once a day.

E. IGS GIMs

The well-known [13] GIMs from IGS are derived from actual GNSS observations collected by its global network of receivers. The model consists on a set of IGPs at 450 km height and with a resolution of 2.5 degrees in latitude and 5 degrees in longitude. These ionospheric grid maps are stored in a standard IONosphere map EXchange format (IONEX) defined in [13], with an updating time of 2 hours.

F. EGNOS ionospheric model

These ionospheric corrections are broadcast in real time by European Geostationary Navigation Overlay System (EGNOS). They are available in the region defined by European Civil Aviation Conference (ECAC) [14]. In this case, Satellite-Based Augmentation System (SBAS) receivers apply the Minimum Operational Performance Standards (MOPS) described in [15]. Its Appendix A describes the ionospheric model, which consists in VTEC values on a single-layer grid at a 350 km height. The IGP grid at the equator has 5° spacings in both latitude and longitude, increasing to 10° north and south of 55 degrees in latitude, and finally becoming spaced 90° in longitude between 85 degrees and the poles. The maximum update time interval is five minutes.

III. Ionospheric Test Description

A strategy to test any ionospheric model for satellite-based navigation is proposed using actual carrier-phase measurements. The assessment only requires to precisely know (i.e., to fix) the previously mentioned carrier-phase ambiguity in the geometry-free combination ($BI = B1 - B2$ [9]). Thence, the proposed metric is to fit the model STEC predictions to the geometry-free carrier-phase combination ($LI = L1 - L2$). The ionospheric model under test $STEC_{model}$ shall differ only from the unambiguous ($LI - BI$), in the hardware delays (i.e., a receiver constant K_i plus a satellite constant K^j):

$$STEC^j_{model,i} - (LI^j_i - BI^j_i) = K_i + K^j \tag{4}$$

The K_i and K^j on the right-hand of the previous equation are estimated by a Least Mean Squares (LMS) process. As other DCB tests [16], the rank deficiency is removed by fixing a single receiver bias. In this way, the post-fit residuals obtained after fitting (4) provide a metric to assess the quality of any ionospheric model for GNSS navigation. The residuals will account for any miss-modelling not being assimilated into the receiver and satellite constants.

Notice the global scale of the test, since more than one hundred receivers globally distributed are taken into account in the common K_i constant parameters. Furthermore, both K_i and K^j parameters are fixed over every twenty-four hour data interval, which cannot accommodate miss-modellings linked to the satellite clocks or orbits. Last, mind that no model or ionospheric a-priori information is used within the test. It is directly the predictions of the model under testing which are assessed against actual measurements.

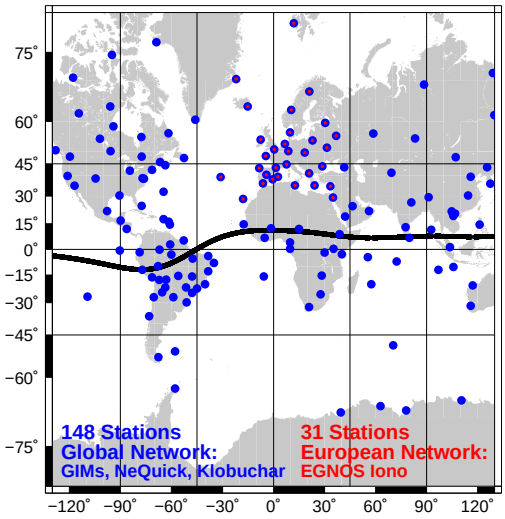

Fig. 1. Distribution of permanent receivers used to asses ionospheric models. The global network shown in blue is used to assess global models such as; GIMs, Klobuchar and NeQuick G. The sub-set of receivers shown in red approximates the EGNOS Ranging and Integrity Monitoring Stations (RIMS) used to derive the EGNOS regional ionospheric model.

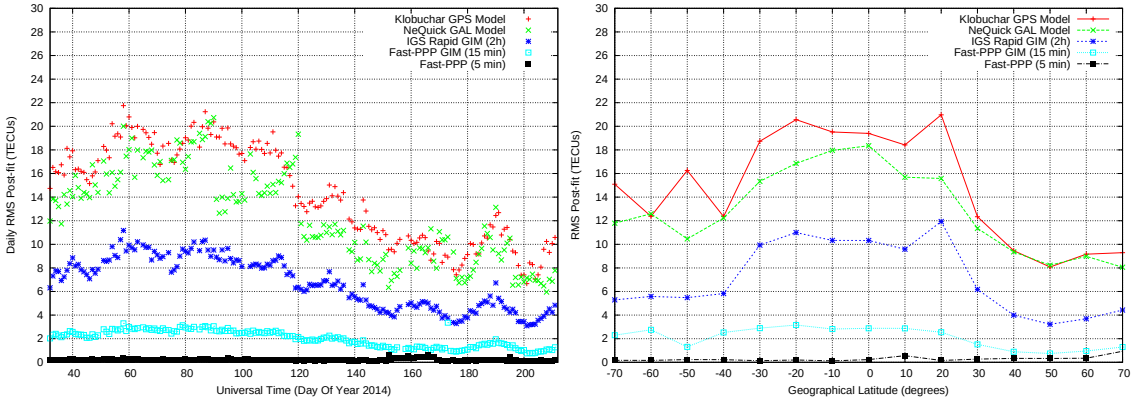

Fig. 2. Results of the consistency test between different global ionospheric estimates; Klobuchar (red) and NeQuick G (green) broadcast models, 2-h Rapid IGS GIMs (dark blue), 15 min Fast-PPP GIMs (light blue), and the real-time (5 min) two-layer Fast-PPP model (black). The horizontal axis is the universal time in the top plot and latitude in the bottom plot.

IV. Global Ionospheric Models Assessment

The test described in Section III has been routinely applied on the global distribution of receivers shown in blue in Fig. 1 for six months starting in February 2014, Day of Year (DoY) 032. After every twenty-four hour of actual GNSS data collection, the $K's$ of adjustment (4) are estimated. Thence, residuals of the fitted $K's$ to the measurements is computed every 5 minutes. The RMS of these post-fit results are grouped in Fig. 2 using two different axes; the Universal Time (UT) in the top plot and the latitude in the bottom.

As it can be seen in Fig. 2, the error of STECs modelled with NeQuick G (green) or Klobuchar (red) predictions can range from 8 TECUs at mid-latitude regions to more than 20 TECUs at low latitudes. A better STEC modelling is achieved by the Rapid GIMs from IGS [17]. The RMS of the IGS-GIMs (dark blue) values is ranging from around 3 TECUs for mid-latitude to around 10 TECUs for equatorial latitudes. Notice that the test is done over obliquos STECs, so this result is in line with the IGS-GIMs nominal accuracy of 2-8 TECU [17], for the VTEC. Finally, the new GIMs developed for the ICASES project by gAGE/UPC shows a typical error (light blue) of its STEC predictions around 1 to 2 TECU, maintained also at low latitude regions. As explained before, the origin of this GIMs is the Fast-PPP real-time estimates, which have the lowest error (black) of 0.25 TECUs.

V. Regional Ionospheric Models Assessment

Results of previously assessed global ionospheric determinations (Fast-PPP and IGS GIMs, Klobuchar and NeQuick G models) will be assessed strictly for the epochs, stations and satellites for which the EGNOS provides ionospheric corrections following the previously mentioned MOPS standard. After applying the MOPS, 5.99% samples (in a 10.5 million total) are discarded.

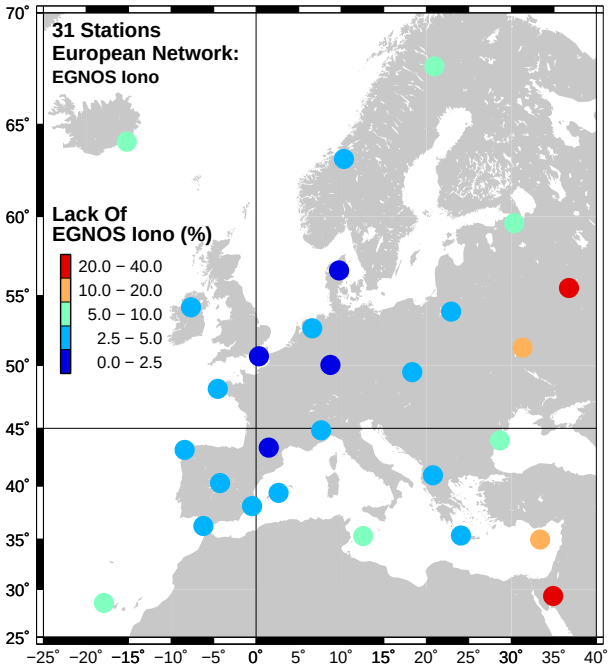

Fig. 3. Distribution of permanent receivers in Europe used to asses EGNOS real-time ionospheric corrections during 6 months starting on DoY 032 of 2014. The unavailability of ionospheric corrections during the assessment is included. It can be seen that mostly occurs in the stations located border of the coverage are, specially in the East region.

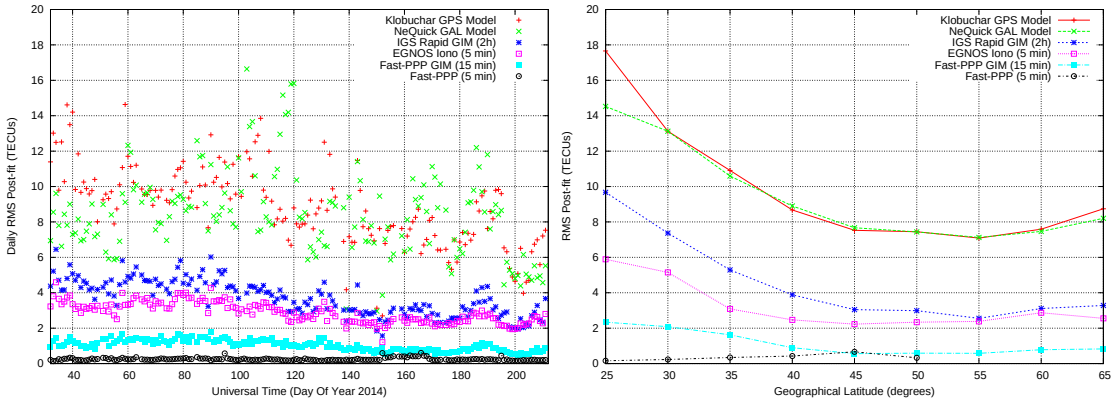

Fig. 4. Results of the consistency test between different regional ionospheric estimates for the ECAC region. Klobuchar (red) and NeQuick G (green) brodcast models, 2-h Rapid IGS GIMs (dark blue), real-time (5 min) EGNOS ionospheric corrections (pink), 15 min Fast-PPP GIMs (light blue), and the real-time (5 min) two-layer Fast-PPP model (black). The horizontal axis is the universal time in the top plot and latitude in the bottom plot.

As it can be seen in Fig. 3, this unavailability of corrections mostly occurs in the stations located border of the coverage are, specially in the East region.

Figure 4 shows the test results for the permanent receivers shown in Fig. 3, covering the ECAC region. As it can be seen, the NeQuick G (green) or Klobuchar (red) model RMS postfit residuals are mostly the same, in the range between 8 to 18 TECUs. The Rapid IGS GIMs (dark blue) present an RMS of 3 to 10 TECUs. The real-time EGNOS ionospheric corrections (pink) are at the level of 2 to 6 TECUs. The aforementioned gAGE/UPC GIMs (light blue) shows the lowest RMS values, with 1 to 2 TECUs. Notice that this GIMs is built from the Fast-PPP model (black) with typical errors well below 1 TECU, maintained also at low latitude regions.

A final remark about the ionospheric test shall be done. This can be understood as the minimum error that the ionospheric corrections will present. On top of this, the interpolation error will degrade the results on the models based on grid (GIMs, EGNOS). This will depend of the distance from the stations used to derive every ionospheric model to the actual IPP of the users.

VI. Differential Code Biases Test Description

The DCBs are instrumental delays occurring at the hardware of both the transmitters and the receivers. The DCBs are different on each frequency, so they must be taken into account when working with different frequencies or, equivalently, one has to consider different clock bias for each frequency. The DCBs can be calibrated on the ground using an anechoic chamber. However, these original values may evolve during the transmitter or receiver life-cycle. Under such circumstances, they shall be re-estimated.

In fact, the operational determination of DCBs is done jointly with the ionospheric models. Thence, the accuracy of the ionospheric modelling affects the precision and stability of the satellite and receiver DCBs determinations. Indeed, the ionospheric combination of code pseudorange measurements ($PI = P_2 - P_1$), for any transmitter j and any receiver i, can be written as:

$$PI = STEC_i^j + DCB_i - DCB^j \tag{5}$$

Some IGS analysis centres estimate the receiver DCB_i and satellite DCB^j biases at the same time than the ionospheric delay $STEC_i^j$, using previous equation, and actual GNSS data from a network of global receivers (see, for instance, [7]). Other IGS analysis centres, estimate these DCBs after deriving their ionospheric model (see, for instance, [1]). Then, using a LMS process, the DCBs are fitted to the code measurements using (5), after removing the ionospheric prediction. This last procedure is also used in [16] for estimating the DCBs of GPS and Galileo satellites.

[18] The DCBs are assessed following a similar procedure to the one previously explained in Section III for the ionosphere. The first difference with respect to (4), is that we now use the code pseudorange measurements. Specifically, we have only used receivers with consistent P1 and P2 measurements (C1W and C2W). In other words, we have excluded the C1C measurements to avoid dealing with the P1-C1 bias. The second difference is that now we are interested in the value of the estimated DCBs (again, a receiver constant K_i plus a satellite constant K^j):

$$STEC_{model,i}^j - PI_i^j = K_i + K^j \tag{6}$$

It is clear from previous equation that the quality and characteristics of the ionospheric model $STEC_{model,i}^j$ will be translated to the DCBs estimations. These K_i and K^j on the right-hand of (6) are estimated, by a LMS process, after every hour of actual GNSS data collection. A third and final difference is that we have constrained to zero the average value of the satellite DCBs, as it is done in the IGS estimation. It will be shown that the stability of the estimated DCBs can be used as an additional indicator of the ionospheric model performance.

VII. Satellite and receiver DCB Assessment

Following the test described in Section VI, we have estimated the DCBs during the period of days 032-212 on 2014 using (6). In Fig. 5 we depict the hourly estimation of the DCBs using the Rapid IGS GIMs ionospheric model and the 2-layer Fast-PPP model. The top plot shows 2 representative satellites and the bottom plot shows 2 representative receivers (KOUR at low latitude and ALAC at mid latitude).

In the top plot of Fig. 5, it can be seen that both ionospheric models (i.e., IGS and Fast-PPP) provide a similar mean determination for the satellite DCBs. This is a consequence of imposing the satellite DCB mean value to zero. However, it must be noted that the Fast-PPP model provides a satellite DCB estimation with a standard deviation clearly lower than the IGS GIMs. Numerically, a factor 3 of difference (0.46 vs 1.22 nanoseconds). This factor is in line with the improvement seen in the results of the ionospheric assessment described in previous Section V and Section IV.

In the bottom plot of Fig. 5, receiver DCB estimates are depicted. A bias appears in both station DCB between both ionospheric models, as a result of the different model geometries and having constrained to zero the average of the DCBs for the satellites. Moreover, in the receiver KOUR receiver, located at an equatorial latitude (5.21° North), an artificial trend appeared, related with the miss-modellings of IGS-GIMs ionospheric model shown in previous sections. The mid-latitude receiver ALAC (38.15° North) the standard deviation differs by a factor 4 (3.03 vs 0.74 nanoseconds) between IGS GIMs (red) and Fast-PPP model (blue).

VIII. Detection of An Actual DCB Drift

This section presents that the quality of the Fast-PPP GIMs is enough for detecting anomalies on satellite or receiver hardware delays. In this sense, an actual drift in the DCB occurring on a permanent receiver of the IGS network can be monitored. This drift can be seen in the top plot of Fig. 6, directly using the code and carrier-phase geometry-free combination of measurements of the adis station for different satellites. For that day, around 8.30h an actual bias of about 50 cm (~1.67 ns) occurs, disappearing six hours later in a similar manner, around 13.30h. This occurs for all satellites in view, whereas in the plot the satellites with the highest elevation are selected in order to show the lowest noise.

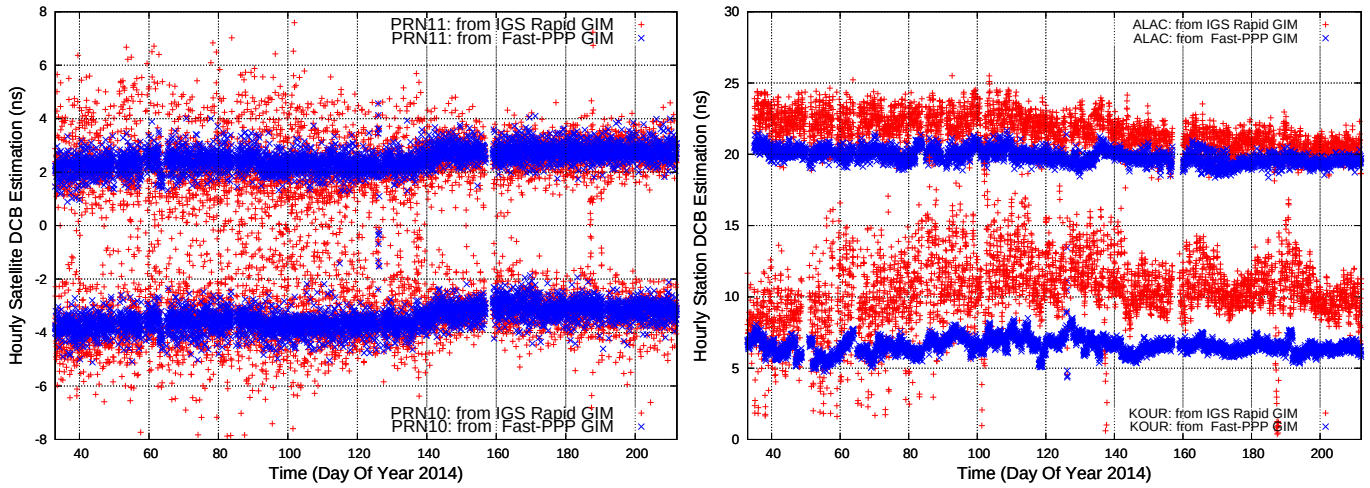

Fig. 5. 6 months of Differential Code Bias (DCB) estimates for satellites (top) and stations (bottom) using different global ionospheric models; 2-h Rapid IGS GIMs (red) and 15-min Fast-PPP GIMs (blue).

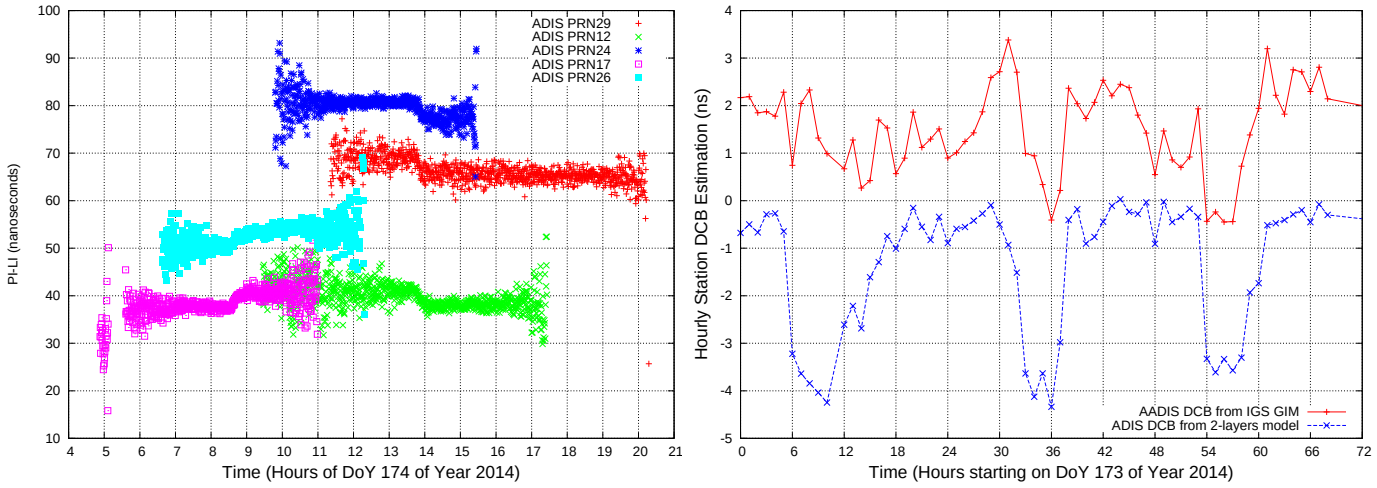

Fig. 6. A drift in the DCB for the International GNSS Service (IGS) receiver ADIS, located at (38.77° W, 8.98° North) can be seen using the geometry-free combination of code and carriers (top plot). The drift occurs daily around 9h and at 14h. The DCB estimation for the adis station is shown in the bottom plot using the Fast-PPP ionospheric model (blue) and the Rapid GIMs from IGS in red.

The bottom plot of Fig. 6 depicts the estimation of the adis station DCB using the aforementioned ionospheric models; Fast-PPP and Rapid GIMs from IGS. These drifts can be detected using the gAGE/UPC ionospheric model. As it can be seen, this event lasts approximately 6 hours and occurs the day before (173) and the day after (175). On the contrary, the level of model error present in other ionospheric models, like the IGS GIMs, does not would allow its detection.

IX. Conclusions

A procedure for assessing the quality of ionospheric models for GNSS has been presented. This test is based on actual carrier-phase measurements. The strategy has been routinely applied for 6 months from February 1, 2014. It has been shown, using this assessment, the planetary performance of the ionospheric models available in real time (NeQuick G for Galileo, and Klobuchar for GPS) to be comparable. The RMS of the ionospheric error is at the level of 8 to 20 TECUs, in mid- and low-latitude regions, being NeQuick G around 2 TECUs better. Second, two post-process global ionospheric models are compared. The Rapid product from the IGS and a new product developed by gAGE/UPC. It has been shown that the accuracy of the IGS-GIMs is between 4 and 12 TECUs, in mid- and low-latitude regions, whereas the GIMs from gAGE/UPC is kept at the level of 2 TECUs for all latitudes. Third, two real-time corrections have been assessed; the EGNOS and the Fast-PPP. While EGNOS shows a 2 to 6 TECUs error in its mid-latitude operation area, the Fast-PPP model accuracies are at the level of a 0.25 TECUs for a planetary coverage.

A second test has been presented to assess the DCB, which are intrinsically determined together with any ionospheric model. Again, the test uses actual code measurements. It has been shown that the satellites biases determined with the ionospheric model derived by gAGE/UPC are typically three times more accurate than the same biases determined with the GIM model

from IGS. This different behaviour is enlarged when the station DCBs are considered. Not only the dispersion gets bigger but also the DCB determinations are biased for the IGS-GIMs. This is particularly noticeable in low-latitude receivers, showing a degradation in line with the results of the ionospheric model assessment previously described. Finally, an additional usage of the precise ionospheric modelling achieved by the Fast-PPP-GIMs is presented, where an actual DCB drift on an IGS permanent receiver can be detected.

ACKNOWLEDGMENTS

The authors acknowledge the use of data from the International GNSS Service and the Centre National d'Études Spatiales (CNES). This work has been financially supported by the ESA/ESTEC project ICASES [3].

REFERENCES

[1] R. Orús, M. Hernández-Pajares, J.M Juan, J. Sanz, and M. García-Fernández, "Validation of the GPS TEC maps with TOPEX data," *Advances in Space Research*, vol. 31, no. 3, pp. 621–627, 2003.

[2] L.-L. Fu, E. J. Christensen, C. A. Yamarone, M. Lefebvre, Y. Mnard, M. Dorrer, and P. Escudier, "TOPEX/POSEIDON mission overview," *Journal of Geophysical Research: Oceans*, vol. 99, no. 12, pp. 24 369–24 381, 1994.

[3] European Space Agency (ESA/ESTEC), "ICASES: Ionospheric Conditions and Associated Scenarios for EGNOS Selected from the last Solar Cycle. PO1520026618/01." Noordwick, The Netherlands, 2014.

[4] A. Rovira-Garcia, M. Juan, and J. Sanz, "A Real-time World-wide Ionospheric Model for Single and Multi-frequency Precise Navigation," in *Proceedings of 27th International Technical Meeting of The Satellite Division of the Institute of Navigation*, Tampa, Florida (USA), Sep. 2014.

[5] IGS Real Time Pilot Project, "http://www.rtigs.net," Jan. 2014.

[6] G. Beutler, M. Rothacher, S. Schaer, T. Springer, J. Kouba, and R. Neilan, "The International GPS Service (IGS): An interdisciplinary service in support of Earth sciences." *Advances in Space Research*, vol. 23, no. 4, pp. 631–653, 1999. [Online]. Available: http://www.sciencedirect.com/science/article/pii/S027311779900160X

[7] A. J. Mannucci, B. D. Wilson, D. N. Yuan, C. H. Ho, U. J. Lindqwister, and T. F. Runge, "A global mapping technique for gps-derived ionospheric total electron content measurements," *Radio Science*, vol. 33, no. 3, pp. 565–582, 1998. [Online]. Available: http://dx.doi.org/10.1029/97RS02707

[8] M. Juan, M. Hernández-Pajares, J. Sanz, P. Ramos-Bosch, A. Aragon-Angel, R. Orus, W. Ochieng, S. Feng, P. Coutinho, J. Samson, and M. Tossaint, "Enhanced Precise Point Positioning for GNSS Users." IEEE Transactions on Geoscience and Remote Sensing *10.1109/TGRS.2012.2189888*, 2012.

[9] J. Sanz, J. Juan, and M. Hernández-Pajares, GNSS Data Processing, Vol. I: Fundamentals and Algorithms. Noordwijk, the Netherlands: ESA Communications, ESTEC TM-23/1, 2013.

[10] J. Juan, A. Rius, M. Hernández-Pajares, and J. Sanz, "A two-layer model of the ionosphere using global positioning system data," *Geophysical Research Letters*, vol. 24, no. 4, pp. 393–396, 1997.

[11] J. Klobuchar, "Ionospheric Time-Delay Algorithms for Single-Frequency GPS Users." IEEE Transactions on Aerospace and Electronic Systems, vol. AES-23, no. 3, pp. 325–331, 1987.

[12] R. Prieto-Cerdeira, R. Orús-Pérez, E. Breeuwer, R. Lucas-Rodriguez, M. Falcone, "The European Way: Assessment of NeQuick Ionospheric Model for Galileo Single-Frequency Users," *GPS World*, vol. 25, no. 6, pp. 53–58, 2014. [Online]. Available: http://gpsworld.com/innovation-the-european-way

[13] S. Schaer, W. Gurtner, and J. Feltens, "IONEX: The IONosphere Map Exchange Format Version 1," in *Proceeding of the IGS AC Workshop*, Darmstadt, Germany, Feb. 1998, pp. 233–247.

[14] "Constitution and Rules of Procedure of the European Civil Aviation Conference (ECAC)," Dec. 1955.

[15] RTCA-MOPS, "Minimum Operational Performance Standards for Global Positioning System/Wide Area Augmentation System Airborne Equipment.rtca document 229-C," Washington, USA, 2006.

[16] O. Montenbruck, A. Hauschild, and P. Steigenberger, "Differential Code Bias Estimation using Multi-GNSS Observations and Global Ionosphere Maps," *Navigation*, vol. 61, no. 3, pp. 191–201, 2014. [Online]. Available: http://dx.doi.org/10.1002/navi.64

[17] IGS Products, "http://www.igs.org/products/data," Jan. 2014.

[18] O. Montenbruck, P. Steigenberger, R. Khachikyan, G. Weber, R. Langley, M. Mervart, and U. Hugentobler, "IGS-MGEX, Preparing the Ground for Multi-Constellation GNSS Science," *Inside GNSS*, vol. 9, no. 1, pp. 42–49, 2014.